*Electrochemical and Solid-State Letters,* **10** (3) H98-H100 (2007)
1099-0062/2007/10(3)/H98/3/$20.00 © The Electrochemical Society

# Structural Properties of ZnO Grown on GaN/Sapphire Templates

## The Transition from Nanorods to Thin Films

**H. L. Zhou,[a] S. J. Chua,[b] H. Pan,[a] J. Y. Lin,[a] Y. P. Feng,[a] L. S. Wang,[b] W. Liu,[b] K. Y. Zang,[b] and S. Tripathy[b,*,z]**

[a]*Department of Physics, National University of Singapore, 119260 Singapore*
[b]*Institute of Materials Research and Engineering, 117602 Singapore*

ZnO nanorods were synthesized on GaN/sapphire substrates using a modified thermal-evaporation process. The as-synthesized ZnO nanorods and thin films were characterized using scanning electron microscopy, micro-Raman, and X-ray diffraction techniques. The morphology of the ZnO changes from nanorods to continuous thin films when the growth temperature increases to 800°C. Further increase in the growth temperature leads to a lower growth rate of ZnO along the (0001) direction. Micro-photoluminescence measurements show ultraviolet band-edge emission peaks around 378 nm from both nanorods and thin films. Realization of such ZnO structures may be useful for the fabrication of hybrid ZnO/GaN optoelectronic devices.
© 2007 The Electrochemical Society. [DOI: 10.1149/1.2428413] All rights reserved.

Manuscript submitted September 12, 2006; revised manuscript received October 27, 2006.
Available electronically January 8, 2007.

ZnO has attracted considerable attention over the past years owing to its attractive properties, such as good piezoelectric characteristics, chemical stability, and biocompatibility, and its potential applications in optoelectronic switches, high-efficiency photonic devices, near-UV lasers, and complex three dimensional nanoscale systems.[1-4] Recently, a number of methods have been used to produce one-dimensional (1D) ZnO nanostructures, such as thermal evaporation, vapor-phase transport, laser ablation, metallorganic chemical vapor deposition, and template-assisted and solution processes.[5-10] For the case of ZnO nanoarray light emitters based on quantum confinement effect, a big challenge is to control the dimension of ZnO nanostructures. Furthermore, the difficulty of p-type doping in ZnO has impeded the fabrication of ZnO homojunction devices. As an alternative approach to homojunction, an n-ZnO/p-GaN heterojunction has been suggested as a strong candidate for device applications.[11,12] Both ZnO and GaN have a fundamental bandgap energy in the range of about 3.3–3.4 eV, with the same Wurtzite crystal structure, and a low lattice misfit of about 1.9%. Recently, Park and Yi reported on the fabrication of n-ZnO/p-GaN nanorod electroluminescent devices and demonstrated the potential to realize photonic and electronic nanodevices.[13] It is a challenge for researchers to achieve large area well-aligned nanostructures by the other cost-effective growth method rather than selective area metallorganic chemical vapor deposition (MOCVD) growth. In this paper, we have shown that ZnO nanorod arrays can be grown on GaN/sapphire (0001) substrates in a controllable way using a thermal evaporation technique. The transition of nanorod morphology to thin film can be achieved by the one-step growth without any interruption and temperature regulation during continuous thermal vaporization process. The crystalline and optical properties of such ZnO structures have been addressed.

GaN films about 4.0 μm thick were first deposited by MOCVD on *c*-plane sapphire substrates with low-temperature GaN buffer layers. Trimethylgallium and ammonia ($NH_3$) were used as the sources of Ga and N, respectively, with $H_2$ as carrier gas. The GaN/sapphire templates were then placed inside a tube furnace for the growth of ZnO films by thermal vaporization of Zn (99.9% purity) powder and subsequent condensation of Zn vapor in the presence of oxygen. The alumina boat with Zn powder was placed at the center of a quartz tube and purged by He (99.999% purity) at a flow rate of 100 sccm. The furnace temperature was increased to the growth temperature in the range of 750–850°C and oxygen (99.99% purity) was introduced in the tube reactor at a flow rate of 10 sccm. The mixed $O_2$ and He gas flow was maintained throughout the whole reaction process ( ~30 min). The morphology of the ZnO/GaN/sapphire samples was studied using a JSM-6700 field-emission scanning electron microscope (SEM). High-resolution X-ray diffraction (HR-XRD) measurements were also performed using a Philips X'Pert X-ray diffraction apparatus equipped with a Cu Kα radiation source. The PL spectra were recorded at room temperature using the 325 nm excitation line (Renishaw 2000 micro-PL-Raman set up) from a He-Cd laser. Micro-Raman measurements were carried out using a JY-T64000 set up equipped with the 514.5 nm excitation line from an Ar ion laser.

The effects of the growth temperature on the morphology of ZnO grown on GaN were systematically studied. In this modified thermal evaporation process, the growth of ZnO is believed to be dominated by the vapor–solid (VS) process. Figure 1 shows the cross-sectional and top view SEM images of ZnO structures grown at different processing temperature. We can clearly see that morphological changes can be controlled by a slight variation of the growth temperature with the availability of Zn-O vapor. When the temperature is lower than 800°C, the as-grown ZnO forms long and needle-shaped nanorods on GaN with a typical average diameter of about 100 nm (see Fig. 1a for 780°C growth temperature). Moreover, the thickness of these nanorods became smaller when the growth temperature increased to 790°C. The observed surface morphology can be explained by a higher growth rate of ZnO along the *c*-direction and the poor surface migration of Zn atoms on (0001) surface at low temperatures. With a further increase in the growth temperature to 800°C, we have seen a quite uniform and continuous ZnO film (Fig. 1b). Formation of a film at this growth temperature could be due to a faster diffusion of the Zn-O vapor and higher surface mobility. However, the window of the growth temperature is small and with a proper choice of the gas flow rates, a smooth ZnO(0001) surface can be achieved. Furthermore, at a much higher growth temperature of 820°C, the ZnO(0001) surface became rough due to the increase in the evaporation rate of absorbed source molecules on the surface (Fig. 1c). Figure 2 shows the effect of the temperature on the growth rate of ZnO with the oxygen flow rate kept at 10 sccm. We can see that higher temperature suppresses the growth rate along the [0001] direction, and led to formation of thin films rather than nanorods.

Figure 3 shows the HRXRD 2ω/θ scans of the ZnO samples grown at different growth temperatures. Here, we have shown the ZnO(0004) and GaN(0004) diffraction peaks that indicate the *c*-axis-oriented ZnO growth with Wurtzite structure. XRD rocking curves were measured to determine the degree of alignment to the

* Electrochemical Society Active Member.
z E-mail: tripathy-sudhiranjan@imre.a-star.edu.sg

Downloaded 20 Jan 2010 to 159.226.100.225. Redistribution subject to ECS license or copyright; see http://www.ecsdl.org/terms_use.jsp

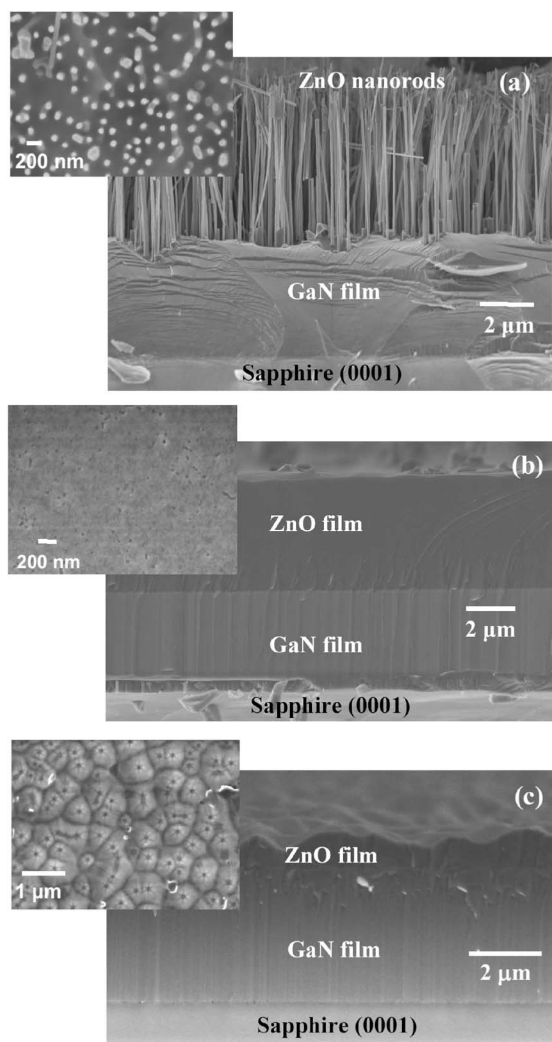


**Figure 1.** Cross-sectional SEM images of the ZnO structures grown on GaN(0001) at different growth temperature with 10 sccm oxygen flow rate. Growth temperature (a) 780, (b) 800, and (c) 820°C. The SEM images in the inset show the top surface morphology.

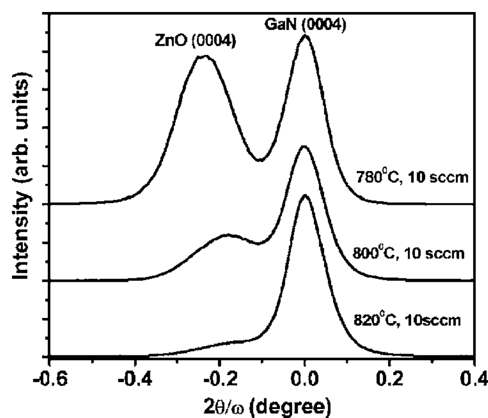


**Figure 3.** (a) The HRXRD ω/2θ scans of the ZnO/GaN/sapphire (0001) heterostructures grown at different temperature.

normal direction of the substrate surface. The narrower full width at half-maximum (fwhm) implies that ZnO nanorods are well oriented along the (0001) direction with improved crystalline properties. The orientation and uniformity of the nanorods prepared by this method are somewhat better than those directly grown on ZnO substrates.[14] Furthermore, the intensity of the ZnO(0004) diffraction peak decreases as the growth temperature increases, indicating a better crystalline quality nanorods when compared to the thin films possessing a large density of point and line defects. A reduction in the thickness of the films also led to a decrease in the XRD peak intensity. From Fig. 3, we can also observe that the ZnO(0004) spectrum from the nanorods structure show a substantial peak shift when compared to the thin films. This is caused by the strain relaxation in nanorod structures because of the aspect ratio.[15] However, the ZnO thin film samples show an in-plane tensile stress component as confirmed from XRD analysis.

The optical properties of the ZnO samples grown on *c*-GaN were investigated by room temperature micro-PL spectroscopy. Figure 4 shows the PL spectra of ZnO samples where the ratio of GaN peak intensity to that of ZnO varies with the growth temperature. This change in the PL spectra indicates a different thickness or/and crystalline quality of ZnO layers. In the PL spectra, the near-band-edge PL peaks from GaN and ZnO nanorods are centered around 363 and 378 nm, respectively. From the continuous ZnO film, the PL appears from the top ZnO surface due to the limitation in the laser penetration depth. Although the absorption coefficient at 325 nm is large in bulk ZnO and GaN, we can assume that laser probing depth in nanorods is somewhat close to the bulk values. In bulk ZnO, due to a wide range of absorption coefficients reported in literature, we have estimated a penetration depth in the range of 60–120 nm under 325 nm excitation. Although the estimated PL probing depth is be-

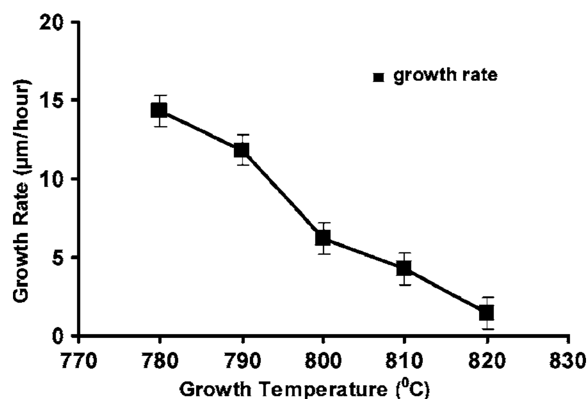


**Figure 2.** The estimated ZnO(0001) growth rate as a function of growth temperature.

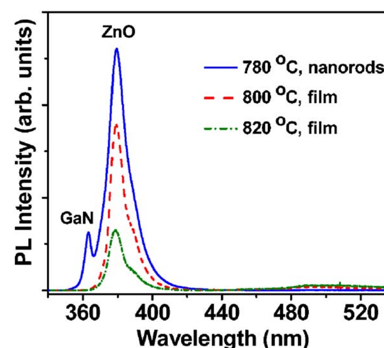


**Figure 4.** The PL spectra recorded from ZnO/GaN samples grown at different temperature with the same oxygen flow rate of 10 sccm. The PL excitation wavelength was 325 nm and the laser power on the sample surface was kept below 0.5 mW.

Downloaded 20 Jan 2010 to 159.226.100.225. Redistribution subject to ECS license or copyright; see http://www.ecsdl.org/terms_use.jsp

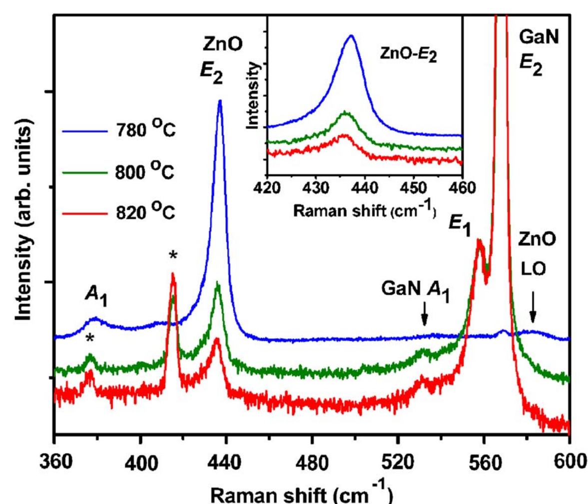


**Figure 5.** Room-temperature Raman spectra of ZnO nanorods (grown at 780°C) and thin films (grown at 800 and 820°C). The spectra were recorded using a $z(xx)\bar{z}$ scattering geometry. The Raman peaks from sapphire substrate are marked by asterisks. The inset shows the $E_2$ phonon peak shift in these ZnO structures.

low 150 nm for bulk GaN, micro-PL signal from underlying GaN appears due to presence of air gaps between ZnO nanorods. For the case of ZnO film grown at 820°C, the PL spectrum also shows a relatively stronger defect-induced broad green emission. The strongest PL intensity is observed from the nanorods grown at 780°C. This is due to an enhanced light extraction due to multiple scattering at the sidewalls/facets of the nanorods. However, band-edge PL from nanorods shows an inhomogenously broadened lineshape due to a fluctuation of the average rod diameter. In addition, interfacial defects could also broadened the PL lineshape. From the continuous films, the decrease in PL intensity and broadening could be associated with the presence of high-density line defects and vacancy-impurity complexes. Recently, Fonoberov et al.[16] reported a comparative PL study from ZnO quantum dots, nanocrystals, and bulk material. In their report, the room-temperature free exciton peak from bulk ZnO appeared at 3.294 eV whereas PL peaks around 3.250 eV from quantum dots are related to bound exciton transitions. In our case, the PL peak from the ZnO nanorods and thin film grown at 800°C appear at 3.266 and 3.270 eV, respectively. Such a red shift in the PL peak positions from our sample with respect to the bulk ZnO exciton peak could be associated with the presence of a tensile stress component. The room-temperature PL spectra of the ZnO nanorods grown at 780°C show the potential for optoelectronic applications.

Next, we present a micro-Raman study of such ZnO structures grown at different temperatures. Raman scattering has become a popular tool to investigate the electron-phonon interaction and crystalline properties of ZnO thin films and nanostructures.[17-19] Figure 5 shows the Raman spectra recorded from the ZnO nanorods and thin films. Raman spectra show strong $E_2^{(2)}$ phonon peak of ZnO near 437 cm$^{-1}$. Other phonon peaks from the underlying GaN and sapphire substrates are also observed. Due to wide bandgap, such a visible 514.5 nm Raman excitation probes the whole ZnO and GaN layer. Because this excitation wavelength is transparent to both ZnO and GaN, we also observed the Raman peaks form sapphire substrates, which are marked with asterisks in Fig. 5. However, the recorded phonon peak intensity is much higher from nanorods when compared to thin films. This is due to the multiple light scattering at the sidewalls of the nanorods. The presence of a large dielectric contrast in the nanorod arrays also led to the observation of $A_1$(LO) phonon peak of ZnO. Furthermore, the relative $E_2^{(2)}$ phonon peak shift has been used to determine the residual stress in such ZnO structures. The in-plane stress values were estimated from the stress vs $E_2$ phonon peak shift, $\Delta\omega = K\sigma$, where $K$ is the proportionality factor given by 6.7 GPa$^{-1}$ cm$^{-1}$ and $\Delta\omega$ is the observed peak shift with respect to bulk phonon peak. This relationship has been derived using the Raman shift calibration and appropriate phonon deformation potentials reported in literature.[15,20] The elastic modulus of ZnO used to determine the proportionality factor was taken from Ref. 21. For the case of a 300 μm strain-free bulk ZnO substrate, $E_2^{(2)}$ phonon peak appears at 438.5 cm$^{-1}$. The red-shifted $E_2^{(2)}$phonon peak from our ZnO structures clearly showed the presence of an in-plane tensile stress component. The $E_2^{(2)}$ phonon peak was observed at 437.3 cm$^{-1}$ from the as-grown ZnO nanorods grown at 780°C and this indicates a small residual tensile stress of about 0.18 ± 0.03 GPa. From the thin film grown at 800°C, the tensile stress value increased to 0.30 ± 0.03 GPa. Similarly, for the case of ZnO film grown at 820°C, the observed tensile stress was of the order of 0.39 ± 0.03 GPa. The accuracy in the residual stress values is about 30 MPa, which is determined by the spectral resolution (±0.2 cm$^{-1}$) of the Raman instrument.

In summary, we observed a nanorod-to-thin film transition in ZnO grown on GaN/sapphire (0001) substrates by a thermal evaporation technique. Arrays of *c*-axis orientated ZnO nanorods can be achieved with good optical properties. The crystalline quality of the nanorods and thin films were studied by HRXRD, micro-Raman, and PL measurements. Such a method to realize ZnO may provide opportunities for the fabrication of hybrid n-ZnO/p-GaN nanophotonic devices.

## Acknowledgment

The authors acknowledge financial support from the Academic Research Fund, National University of Singapore.

*The Institute of Materials Research and Engineering assisted in meeting the publication costs of this article.*

## References

1. Y. N. Xia, P. D. Yang, Y. Sun, Y. Wu, B. Mayers, Y. Yin, F. Kim, and H. Yan, *Adv. Mater. (Weinheim, Ger.)*, **15**, 353 (2003).
2. Z. W. Pan, Z. R. Dai, and Z. L. Wang, *Science*, **291**, 1947 (2001).
3. J. Hu, T. W. Odom, and C. M. Lieber, *Acc. Chem. Res.*, **32**, 435 (1999).
4. C. S. Chen, C. T. Kuo, T. B. Wu, and I. N. Lin, *J. Acoust. Soc. Jpn.*, **36**, 1169 (1997).
5. M. Huang, S. Mao, H. Feick, H. Yan, Y. Wu, H. Kind, E. Weber, R. Russo, and P. D. Yang, *Science*, **292**, 1897 (2001).
6. Y. C. Kong, D. P. Yu, B. Zhang, W. Fang, and S. Q. Feng, *Appl. Phys. Lett.*, **78**, 407 (2001).
7. J. J. Wu and S. C. Liu, *Adv. Mater. (Weinheim, Ger.)*, **14**, 215 (2002).
8. M. J. Zheng, L. D. Zhang, G. H. Li, and W. Z. Shen, *Chem. Phys. Lett.*, **363**, 123 (2002).
9. G. Z. Shen, Y. Bando, and C. J. Lee, *J. Phys. Chem. B*, **109**, 10578 (2005).
10. Y. B. Li, Y. Bando, and D. Golberg, *Appl. Phys. Lett.*, **84**, 3603 (2004).
11. (a) R. D. Vispute, V. Talyansky, S. Choopun, R. P. Sharma, T. Vekatesan, M. He, X. Tang, J. B. Halpern, M. G. Spencer, Y. X. Li, L. G. Salamanca-Riba, A. A. Iliadis, and K. A. Jones, *Appl. Phys. Lett.*, **73**, 348 (1998); (b) S.-K. Hong, T. Hanada, H. Makino, Y. Chen, H.-J. Ko, T. Yao, A. Tanaka, H. Sasaki, and S. Sato, *Appl. Phys. Lett.*, **78**, 3349 (2001).
12. (a) H. J. Fan, B. Fuhrmann, R. Scholz, F. Syrowatka, A. Dadgar, A. Krost, and M. Zacharias, *J. Cryst. Growth*, **287**, 34 (2006); (b) H. J. Fan, W. Lee, R. Hauschild, M. Alexe, G. Le Rhun, R. Scholz, A. Dadgar, K. Nielsch, H. Kalt, A. Krost, M. Zacharias, and U. Gösele, *Small*, **2**, 561 (2006).
13. W. I. Park and G.-c. Yi, *Adv. Mater. (Weinheim, Ger.)*, **16**, 87 (2004).
14. L. Wang, X. Zhang, S. Zhao, G. Zhou, Y. Zhou, and J. Qi, *Appl. Phys. Lett.*, **86**, 024108 (2005).
15. G. W. Cong, H. Y. Wei, P. F. Zhang, W. Q. Peng, J. J. Wu, X. L. Liu, C. M. Jiao, W. G. Hu, Q. S. Zhu, and Z. G. Wang, *Appl. Phys. Lett.*, **87**, 231903 (2005).
16. V. A. Fonoberov, K. A. Alim, A. A. Balandin, F. Xiu, and J. L. Liu, *Phys. Rev. B*, **73**, 165317 (2006).
17. (a) K. A. Alim, V. A. Fonoberov, M. Shamsa, and A. A. Balandin, *J. Appl. Phys.*, **97**, 124313 (2005); (b) K. A. Alim, V. A. Foroberov, and A. A. Balandin, *Appl. Phys. Lett.*, **86**, 053103 (2005).
18. B. Kumar, H. Gong, S. Y. Chow, S. Tripathy, and Y. N. Hua, *Appl. Phys. Lett.*, **89**, 071922 (2006).
19. V. A. Fonoberov and A. A. Balandin, *Phys. Rev. B*, **70**, 233205 (2004).
20. Th. Gruber, G. M. Prinz, C. Krichner, R. Kling, F. Reuss, W. Limmer, and A. Waag, *J. Appl. Phys.*, **96**, 289 (2004).
21. W. Lee, M.-C. Jeong, and J.-M. Myoung, *Nanotechnology*, **15**, 254 (2004).

**Downloaded 20 Jan 2010 to 159.226.100.225. Redistribution subject to ECS license or copyright; see http://www.ecsdl.org/terms_use.jsp**